Climate Services 16 (xxxx) xxxx

Contents lists available at ScienceDirect

Climate Services

journal homepage: www.elsevier.com/locate/cliser

Original research article

A process-based statistical seasonal prediction of May–July rainfall anomalies over Texas and the Southern Great Plains of the United States

D. Nelun Fernando[a], Sudip Chakraborty[b,*], Rong Fu[b], Robert E. Mace[a,1]

[a] Water Science & Conservation, Texas Water Development Board, Austin, TX, USA
[b] Department of Atmospheric and Ocean Sciences, University of California-Los Angeles, CA, USA

ARTICLE INFO

Keywords:
Drought
Rainfall forecast
Texas
Early warning

ABSTRACT

With the aim of providing actionable drought early warning information that water managers and reservoir operators in Texas could use to implement drought contingency triggers on water supply sources, we have developed a statistical seasonal prediction system using a canonical correlation analysis prediction model to predict rainfall from May through July (MJJ), the main rainfall season over much of Texas and the Southern Great Plains. The statistical model is trained with data between 1982 and 2005 using standardized anomalous geopotential height at 500 hPa, convective inhibition energy, and soil moisture content in April as the predictors to generate tercile categorical forecasts of MJJ rainfall. Based on commonly used forecast skill metrics, this statistical prediction system provides 20–60% higher skill than that obtained from dynamical seasonal forecasts, and the exceeds skill due to the persistence of MJJ rainfall anomalies over Texas, western Louisiana, Oklahoma and the Southern Kansas. 2011 hindcast shows that below-normal MJJ rainfall anomalies comparable to those observed over most of the region. The forecasts for 2014 captured the above-normal MJJ rainfall anomalies as observed in that year. The forecasts since 2014 have shown acceptable prediction skills at one-to-three months' lead-time. We have also extended the lead-time to generate probabilistic MJJ rainfall forecasts from January through March using a hybrid dynamical-statistical forecast scheme. The predictions have been used by the Texas Water Development Board to inform the Texas State Drought Preparedness Council and to support the implementation of drought contingency triggers for water supply sources by stakeholders, such as river authorities.

Practical Implications.

We have developed a hybrid dynamical-statistical rainfall forecast tool to enhance the reliability of the summer drought early warning over Texas and Southern Great Plains region of the United States. May and June are the wettest months across much of Texas and southern Great Plains region. July is the start of the rainfall season for the western part of the state. Failure of the May–July rains is an indicator that Texas is in the throes of a summer drought. Such a drought could worsen in August, generally the driest and hottest month of the year over much of the state. Improving seasonal forecasts of May–July rainfall over Texas thus serves as an early warning of the likelihood of summer drought over the state. Unfortunately, dynamical climate models have virtually no skill in predicting rainfall in this season over Texas and Southern Great Plains (Hao et al., 2018; Infanti and Kirtman 2014; Livneh and Hoerling 2016; Mo and Lyon 2015; Slater et al. 2016). The dynamical-statistical prediction model reported in this study was developed at the request of the Texas Water Development Board. Its predictions have shown to be of direct utility for summer drought early warning over Texas.

The hybrid dynamical-statistical rainfall forecast tool was designed, developed, and tested in collaboration with the Texas Water Development Board, which is the state agency responsible for collecting and disseminating water data, compiling the state water plan based on sixteen regional water plans, and providing low-cost financing for water, wastewater, and flood mitigation projects. The model is based on our previous research, also undertaken in consultation with the Texas Water Development Board, on the predictability of drought over Texas.

The impetus for developing such a tool came on the heels of the 2011 drought over the state, which was the worst one-year drought on record. In response to the 2011 drought over Texas, the Texas Administrative Code § 358.3 (1) on *Guidance Principles for the State Water Plan Development* (http://txrules.elaws.us/rule/

* Corresponding author.
E-mail address: sudipm@ucla.edu (S. Chakraborty).
[1] Current affiliation: The Meadows Center for Water and the Environment, USA.

https://doi.org/10.1016/j.cliser.2019.100133
Received 24 September 2018; Received in revised form 23 August 2019; Accepted 16 October 2019

title31_chapter358_sec.358.3) was modified to state that: "The state water plan shall provide for the preparation for and response to drought conditions". These rule changes require all regional water plans to have a chapter dedicated to drought response information, activities, and recommendations. With these rule modifications, it became a requirement, in 2012, that all regional water planning groups to include a chapter on drought management with the aim of implementing short-term water demand reductions in the face of impending or existing drought conditions. Each water user group in a water planning region is required to develop drought contingency plans and drought action triggers for their respective water supply sources. Water user groups need to consult existing information on impending or current drought conditions before deciding on whether to implement drought contingency triggers, which set in place voluntary or mandatory water use restrictions. Tools such as the May–July seasonal rainfall forecast provide water user groups with information on impending drought conditions. Such information has been used to aid their decisions on whether to plan for short-term water supply reductions.

Given the improvement in prediction skills demonstrated by the hybrid dynamical-statistical forecast, the Texas Water Development Board has been issuing county-level probabilistic rainfall forecasts for the May–July season, based on the hybrid forecast system, since 2016 via https://waterdatafortexas.org/drought/rainfall-forecasts. Archives of probabilistic forecasts and hindcasts of May–July rainfall, obtained using the statistical forecast model, are also available at this website.

In summary, we identified through user consultation, the key season in which having a skillful rainfall forecast would improve decision-making in the water management sector. We worked with an interdisciplinary team that included climate scientists, hydrologists, water managers, river authorities and developers of the scientific applications to provide the rainfall forecast via an interface that decision makers in the water sector across Texas consult for drought information. Through this interface, we have presented the forecast as county-level and Hydrological Unit Code (HUC) level 8 categorical probabilistic rainfall forecasts, and as quantitative forecasts with associated probabilities of exceedance curves so that users, such as reservoir operators, could select the type of forecast information of most relevance to their decision need. We have also provided detailed guidance on what types of information the forecast conveys and a link through which users could submit questions (https://waterdatafortexas.org/drought/rainfall-forecast-info) on the tool. The web interface is constantly being improved with feedback from users such as river authorities in the state. For example, we included the provision of the rainfall forecast by the U.S. Geological Survey's Hydrological Unit Code (HUC) 8 level watershed regions within Texas based on feedback from the Brazos River Authority of Texas. The steps we have taken in designing, testing, sharing, communicating, and improving the rainfall forecast tool conform to the key steps needed for the development of a climate service prototype that is tailored to fit user requirements (Christel et al. 2018).

1. Introduction

The U.S. Southern Great Plains is an important region for food and energy production. The value of agriculture in the region exceeds tens of billions of dollars (Steiner et al. 2018). However, this region is also prone to extreme droughts. Recent studies suggest that strong summer droughts over the U.S. Southern Great Plains (110°W-92°W and 24°N-40°N) are often characterized by a rapid intensification of dryness during late spring – early summer (Fernando et al. 2016). Dynamical climate models could not predict these droughts (Hoerling et al. 2014; Kumar et al. 2013; Seager et al. 2014) two–three months in advance and underestimate rainfall variance (Kam et al. 2014) in part owing to their limitations in representing summertime convection and land-surface feedbacks (Dai and Trenberth 2004; Wang et al. 2015). In fact, three-month lead time seasonal rainfall forecasts from dynamical forecast models show less skill than the autocorrelation of rainfall anomalies (Hoerling et al. 2014; Quan et al. 2012).

Early warnings of May–July (MJJ) rainfall anomalies relative to the historical mean over the Southern Great Plains are essential for drought resiliency planning in agriculture, water management, energy, and forestry, and for supporting emergency management. For example, an improved MJJ rainfall anomalies can enable early initiation of drought protocols for wildfire prevention, stocking up on drinking water supplies, restriction of non-essential water use, early action to curtail evaporative water loss from water supply reservoirs, etc. The improved seasonal prediction of MJJ rainfall anomalies reported in this study enables the stakeholders to implement water conservation, and acquire needed permits and supplies for drought risk reduction and wildfire preparedness planning with one-to-three months' lead-time, which could reduce the economic cost and structural damage from drought and wildfires.

What causes late spring - early summer or MJJ drought over the US Southern Great Plains? Droughts in Texas are generally associated with La Niña-induced cooler sea surface temperature (SST) anomalies (Ropelewski and Halpert 1986, 1987; Schubert et al. 2009). Established in the fall, cooler than normal SST anomalies contribute to winter drought over Texas by causing a poleward displacement of the subtropical jet stream (Eichler and Higgins 2006; Kousky 1989). In addition, Fernando et al. (2016) have observed that dry springs play a pivotal role in the onset of severe-to-extreme summer drought events over Texas and the Great Plains, consistent with past case studies (Namias 1982; Seager et al. 2014). In particular, the advection of warm and dry westerly winds in the lower troposphere from the Mexican plateau in April can increase temperature at 700 hPa, which in turn increases convective inhibition energy (CIN, negative buoyancy in the lower troposphere) (Fernando et al. 2016; Ryu and Hayhoe 2017a,b). These factors inhibit the development of convective systems during the onset of summer rainfall and are the main contemporaneous cause of drought during June through August over Texas (Fernando et al. 2016; Myoung and Nielsen-Gammon 2010a). Thus, these studies concluded that an enhanced CIN in the spring is an important precursor for summer drought over the region.

Only half of the La Niñas lead to summer droughts over the US Great Plains (Pu et al. 2016). Thus, La Niña alone is not a good predictor of the summer droughts. Rather, Fernando et al. (2016) shows that about 12 out of 13 summer droughts over the US Great Plains since 1950 were preceded by a dry spring. They attribute such a spring to summer memory to land surface feedbacks, based on many previous studies (Hong and Kalnay 2002; Lyon and Dole 1995). For example, Koster et al. (2004) using simulations show that soil moisture and precipitation are strongly coupled over the Central United States, including the Southern Great Plains. The lack of precipitation from winter through early-spring leads to significant cumulative soil moisture deficits, a reduction in evapotranspiration, and an increase in sensible heating as well as surface temperature to balance the decrease of evapotranspiration (Fernando et al. 2016). Dry soil owing to the precipitation deficit provides a positive feedback and further enhances such deficits (Mueller and Seneviratne 2012). Such a positive land surface feedback manifests itself as a significant correlation between dry soil moisture anomalies and lagged 500 hectoPascals (hPa) geopotential height anomalies (2–3 weeks) over the South-Central United States (Fernando et al., 2016). In addition to the local feedbacks, a persistent westward expansion of the North Atlantic Subtropical High over the region could suppress convection over the region (Ryu and Hayhoe 2017b). Dry soil moisture, reduced cooling owing to evapotranspiration along with a high pressure raise the surface temperature, convective inhibition over the domain and lead to a reduction in precipitation.

This study aims to apply the above discussed predictive understanding to improve probabilistic prediction of MJJ rainfall anomalies by introducing a statistical forecast system based on multivariate

Empirical Orthogonal Function (EOF) and Canonical Correlation Analysis (CCA) provided by the Climate Prediction Toolkit (Mason and Tippet, 2016). Our predictor variables are based on our understanding of these key processes responsible for the initiation and persistence of rainfall deficits. We show the sensitivity of our statistical model skills to various input datasets, compare the statistical forecast skill with those of the dynamical forecasts, and assess the skill of hindcasts of MJJ rainfall anomalies for known dry and near-normal years over Texas and the Southern Great Plains region. We also discuss the steps we took to provide the forecasts from our statistical model through a website that was designed and updated with continuous user feedback.

2. Datasets

We used monthly 1°x1° rainfall from the CPC global land precipitation dataset (Chen et al. 2002) to derive seasonal rainfall for the period 1982–2014 (https://www.esrl.noaa.gov/psd/data/gridded/data.unified.daily.conus.html).

We also used anomalous monthly 500 hPa geopotential height, temperature at 700 hPa, 2-meter dewpoint temperature and 0–10 cm depth liquid volumetric soil moisture (non-frozen) for March, April, and March-May (MAM) from the National Centers for Environmental Prediction (NCEP) Climate Forecast System Reanalysis (CFSR) for the period of 1982–2010 (Saha et al. 2010), and the monthly values of the same fields derived from the 6-hourly Climate Forecast System version 2 (CFSv2) real-time data for the period 2011–2014 (Saha et al. 2014). These CFSR and CFSv2 data are obtained from the Data Library of the International Research Institute for Climate and Society (http://iridl.ldeo.columbia.edu).

The latitudinal means were removed from the 500 hPa geopotential height data. CIN is calculated by subtracting temperature at the 700 hPa pressure level from 2 m dew point temperature following (Myoung and Nielsen-Gammon 2010b).

To test the sensitivity of the prediction skills to the uncertainty of data for the predictors, we used 500 hPa geopotential height and temperature at 700 hPa from monthly means of analyzed state meteorology product (MAIMNPANA, https://cmr.earthdata.nasa.gov/search/concepts/C1274767784-GES_DISC); relative humidity and air temperature at 925 hPa from the 3-hourly instantaneous meteorology product (MAI3CPASM); and root zone soil wetness data from the monthly mean land surface diagnostics product (MATMNXLND) for April 1982–2013 from the National Aeronautics and Space Administration (NASA) Modern Era Retrospective-analysis for Research and Applications (MERRA) (Rienecker et al. 2011). Monthly dew point is derived using the 3-hourly relative humidity and air temperature fields. The latitudinal means are removed from the 500 hPa geopotential height data. MERRA reanalysis is available at OPeNDAP/DODS access to the NASA GES DISC GrADS data server (https://goldsmr3.gesdisc.eosdis.nasa.gov/opendap/).

To test the sensitivity of the prediction skill to soil moisture input and the potential improvement of prediction skill using satellite observations of the soil moisture anomalies, we also used daily soil moisture, aggregated to monthly values, from the merged active and passive microwave retrievals product of the European Space Agency Climate Change Initiative Essential Climate Variable Soil Moisture (ECV-SM) dataset version 1 (http://www.esa-soilmoisture-cci.org; (Liu et al., 2011, 2012) for the period 1982–2010. These data are available at 25 km resolution.

To compare the skills of the statistical prediction model to those of the ensemble seasonal prediction by dynamical models, we obtained the ensemble mean rainfall predictions of all the ensemble members (listed in parentheses) of seven models that participated in the North American Multi-model Ensemble Project (NMME, Kirtman et al., 2014). These models are the CMC1-CanCM3 (10), CMC2-CanCM4 (10), COLA-RSMAS-CCSM3 (6), GFDL-CM2p1-aer04 (10), GFDL-CM2p5-FLOR-A06 (12), NASA-GMAO-062012 (12), and CFSv2 (28). The skills of these ensemble rainfall predictions for MJJ during the period of 1982–2010 are compared to those of the statistical prediction. These can also be downloaded from http://iridl.ldeo.columbia.edu.

All data fields cover the domain 24°N-40°N and 110°W to 92°W, referred to in this study as the Texas and Southern Great Plains domain. All the data fields were gridded to 1° horizontal resolution using bilinear interpolation.

3. Statistical prediction tool and forecast products

3.1. Computing the predictor and predictand inputs for the statistical forecast model:

We use datasets over a period of 1982–2005 to train the statistical prediction model. First, we convert all the predictor variables (CIN, soil moisture, and 500 hPa geopotential height) into standardized anomalies to highlight the rainfall anomalies relative to their local variability and to minimize the impacts of data biases. The predictor variables are subjected to multivariate EOF analysis using the Singular Value Decomposition (SVD) algorithm. Multivariate EOF of the predictor variables enables the extraction of the most coherent spatial and temporal variances in a dataset (Lorenz 1956) and maximize the explained covariance. The leading modes of the multivariate EOF analysis capture the largest co-variability found in the original dataset (Wilks, 2006). We retained the first two EOF modes, accounting for at least 70 percent of the variance in the predictor fields. We then applied the Varimax method (Kaiser 1958) to rotate the first two multivariate EOF modes (Richman 1986). The rotated EOF modes are linear combinations of the two orthogonal multivariate EOF modes and represent interrelated clusters (Barnston and Livezey 1987) of the predictor fields. The code is available at https://github.com/twdb/wdft-drought/tree/master/data and can be accessed by sending a permission request to waterdatafortexas@twdb.texas.gov.

We use standardized anomalous soil moisture, geopotential height, and CIN during April as inputs to the CCA statistical model for predicting rainfall in late spring - early summer (May-July, or MJJ). The monthly standardized anomaly at each grid point was calculated by subtracting the monthly mean for a given month from the observed value at a grid point and, then dividing by the monthly standard deviation for that grid point. Each grid point has twelve monthly means and standard deviations, respectively. This method of deriving monthly anomalies removes seasonality.

We input the spatial loadings of the rotated multivariate EOF modes as predictor variables to a Canonical Correlation Analysis (CCA) (von Storch and Zwiers, 2002) using the Climate Predictability Tool (CPT, http://iri.columbia.edu/our-expertise/climate/tools/cpt/, (Mason and Tippet 2016; Simon J. Mason 2017). To compute the skills and the probabilities of the occurrences of drought, we have used CPT version 14. We have also undertaken the analysis using CPT versions 14 and 15. Therefore, the analysis can be replicated using the latest CPT version. We arrange the yearly rotated values for the first two modes and use as X input to the CPT. For Y input, we use the chronological rainfall values for May-June period. CCA maximizes the correlations between the principal components of the leading multivariate EOF of the predictors and the principal components of the predictand. In doing so, it identifies a sequence of pairs of patterns between the predictors and the predictand fields (Wilks 2006). CCA has been shown to be an effective approach for forecasting SSTs (Landman and Mason 2001), seasonal temperatures over land (Shabbar and Barnston 1996), and ENSO episodes (Barnston and Vandendool 1993). Thus, we choose CCA for constructing our statistical model for seasonal forecast of MJJ rainfall anomalies.

3.2. Hybrid dynamical-statistical forecast

For the hybrid dynamical-statistical forecast, we use forecasts of

predicted values of April atmospheric circulation patterns and soil moisture over Texas known to influence May–July rainfall at 3-month (January), 2-month (February), and 1-month (March) lead times. The predictions are obtained from the Climate Forecast System version 2 (CFSv2, Saha et al., 2014), which is the operational dynamical seasonal forecast model of the National Oceanic and Atmospheric Administration-National Centers for Environmental Prediction. The hybrid dynamical-statistical forecast is based on the Model Output Statistics where there is a lag time between the predictor and the predictand unlike the Perfect Prognosis approach, where the is no lag time between the predictor and the predictand.

3.3. Skill scores

Forecast skill assessment was undertaken using cross-validated forecasts (Barnston and Ropelewski 1992; Michaelsen 1987) over a 24 year training period from 1982 through 2005, with a 3-year cross-validation window. The strength of the predictor fields was assessed based on the goodness-of-fit between the cross-validated forecasts and the observation time series (CPC precipitation measurements). The forecasts are available as deterministic forecasts (i.e. for rainfall anomalies) or as categorical probabilistic forecasts (i.e. probabilities of whether seasonal rainfall will be below-, near-, or above-normal).

Skills of the statistical models are assessed in two steps. First, the skill of deterministic forecasts of seasonal cumulative rainfall is assessed using Spearman's Ranked Correlation between observations and cross-validated rainfall at each grid point. Second, the skill of probabilistic forecasts was assessed using the Two Alternative Forced Choice score for forecast categories (2AFC; (Mason and Weigel 2009), the area under the Relative Operating Characteristics curve for the below-normal category (ROC; (Mason and Graham 2002), and the Ranked Probability Skill Score (RPSS, Muller et al., 2005), again at each grid point. The 2AFC score ranges from 0 to 100 percent. 2AFC scores > 50 percent indicates that the forecast is able to discriminate beyond random guessing (Mason and Weigel 2009). The ROC compares hit rate versus false alarm of the prediction to those of random noise. The area under the curve represents the probability that the prediction is correct beyond that by chance. The RPSS is used to explore how these skill scores compare to the mean square error in a probability space. RPSS is a widely used method to compute skills for ensemble forecasts. RPS is calculated from a cumulative distribution. The difference in the observation and the prediction is squared to calculate the score.

Given our interest in late spring - summer drought early warning, we use the ROC score to assess whether the statistical rainfall forecast is able to correctly discriminate the below-normal forecast category from the near-normal or above-normal forecast categories. The ROC score also ranges from 0 to 1 and only a score > 0.5 indicates that the forecast is able to discriminate beyond random guessing. For the RPSS, we adopted the subjective RPSS threshold of five percent (5%) as representing "good skill" in a forecast after Goddard and Dilley (2005). set a subjective. We have used this threshold in the interpretation of the forecast skill from our statistical model.

To assess if statistical predictions can provide higher skills than those of the dynamical prediction, we also compare 2AFC, ROC, and RPSS for the three-month lead NMME forecasts of MJJ precipitation with those scores obtained from the statistical forecast of MJJ rainfall, both initialized in April. The tercile probabilities for the NMME forecasts were obtained using the GCM validation option in CPT, which lets the user compare model output to observed data either on a station or grid box basis.

3.4. Developing rainfall forecast products of use to Texas stakeholders

The Texas State Drought Preparedness Council, on page 32 of its 2014 Drought Annex (https://www.preparingtexas.org/Resources/documents/State%20and%20Fed%20Plans/2014_04_04_Drought%20Annex.pdf), states that: "Although drought is a slow moving incident, public information on forecasted or persistent drought conditions and impacts is extremely vital. The release of timely, consistent and effective public information helps all Texans understand threats, potential impacts, available services, funding options and timelines for response and recovery." The MJJ rainfall forecast has direct utility to Texas' Drought Annex.

The TWDB is a member of the Texas Drought Preparedness Council and is responsible for providing monthly (or quarterly, if there is no ongoing drought) updates on drought and water supply conditions in the state. It has been providing real-time reservoir storage conditions, drought indices, water supply conditions, etc., via waterdatafortexas.org since 2012. Given that the statistical model could forecast summer rainfall over Texas and the Southern Great Plains region in the spring with skill levels acceptable to decision makers, and because drought resilience within Texas could be enhanced through the provision of advanced information for drought preparedness planning, the TWBD automated the rainfall forecast model and started providing probabilistic forecasts of average May–July rainfall in each county in Texas from the beginning of May 2016. The forecasts were issued from mid-January through May 1 of each year. The forecasts are updated at the beginning and middle of each month using forecasts of April predictors initialized on January 15, February 1, February 15, March 1, and March 15. Forecast updates issued on April 1 and April 15 use reanalysis fields of April predictors from the CFSR dataset. The forecasts are, in effect, be summer drought forecasts at 6.5- and 6-month (January initial conditions), 5.5- and 5-month (February initial conditions), 4.5- and 4-month (March initial conditions), and 3.5 and 3-month (April initial conditions) lead times.

Drought management as a water management strategy is an interim strategy designed to meet near-term needs through demand reduction until long-term water supply measures are implemented. Such a strategy typically targets a reduction in municipal water demand. In the long-term it increases water use efficiency and serves more users. New rules adopted for TWDB's water planning process in 2012 (http://txrules.elaws.us/rule/title31_chapter358_sec.358.3) requires all regional water planning groups to include a chapter dedicated to drought response information, activities, and recommendations. The water planning regions are required to seek better information on drought action-triggers, and to provide recommendations for each existing water source (triggers and responses).

The TWDB collaborated with the Brazos River Authority, a key water management and reservoir operations entity in Texas, to apply the rainfall forecast tool to provide guidance information on the likelihood of reservoir storage dropping below drought trigger levels. This information could set in place drought response stage restrictions as defined in drought contingency plans of water user groups in Texas.

We worked closely with the Brazos River Authority's Water Services (BRA) staff in developing the reservoir storage forecast methodology. Engagement with BRA staff commenced in October 2015 when we asked them if they would be interested in working with the Texas Water Development Board on developing a test scenario of the application of seasonal rainfall forecasts for reservoir storage forecasts. BRA staff was very receptive to our inquiry and was eager to collaborate with us. We met several times with them in person and had frequent communication via e-mail regarding datasets, forecast methodologies, and progress updates. They also helped us identify test reservoirs, explained their information needs related to drought contingency trigger implementation, provided us with historic monthly diversion data for their reservoirs, and provided us with diversion estimates for the forecast seasons.

BRA staff has let us know that they have been tracking the bi-weekly rainfall, and have also let us know that they will be including the rainfall forecast tool as a resource to be checked for drought initiation in their 2019 Drought Contingency Plan revision. We consider their intention to include the tool in their Drought Contingency Plan update

as a major achievement of our effort to develop a climate service for drought early warning in Texas. While working on the experimental reservoir storage forecasts we realized that the probabilistic rainfall forecasts did not provide sufficient information by which to tailor the reservoir forecast. Exceedance probability plots provide information on the probability of exceedance of a particular percentile, or percentage of normal, of rainfall. Such information is useful when designing a reservoir forecast because it provides the user with information about how much drier or wetter a particular season is going to be. Such quantitative (or deterministic) information is more useful to water managers than is information on only the likelihood of whether the seasonal will be above-, near-, or below-normal. Therefore, we developed added functionality to the rainfall forecast tool to include graphs of rainfall exceedance probabilities for each county on the interactive rainfall forecast map. We also included the provision of the rainfall forecast by the U.S. Geological Survey's Hydrological Unit Code (HUC) 8 level watershed regions within Texas based on feedback from the Brazos River Authority of Texas.

4. Results

In Fig. 1 we illustrate the key pre-conditions in spring for MJJ rainfall deficit using the Spearman's rank correlation between MJJ rainfall and different meteorological as well as land-surface parameters in April. Geopotential height anomalies at 500 hPa (Z_{500}) in April are negatively correlated with rainfall anomalies in MJJ centered over the Southern and Western Texas, northern Mexico, and over a large area of New Mexico and Colorado ($p < 0.10$) (Fig. 1a). Such negative correlation suggests that an anomalously high geopotential height at 500 hPa in April is significantly correlated with a negative rainfall anomaly in MJJ. We have also found a similar correlation pattern between the geopotential height at 250 hPa in April (not shown) and rainfall anomalies in MJJ to that shown in Fig. 1a. A significant negative correlation ($p < 0.10$) between the surface temperature anomalies in April and rainfall anomalies in MJJ is seen over Texas, northeastern Mexico, eastern New Mexico and eastern Colorado (Fig. 1b), suggesting that anomalously warm surface temperature in April is correlated with anomalously low rainfall in MJJ over these regions. There is a negative correlation between an increase of CIN in April and decrease of rainfall in MJJ over the Southwestern half of the Texas and Northeastern Mexico (Fig. 1c). Finally, dry soil moisture anomalies in April are significantly correlated with negative rainfall anomalies in MJJ over much of the Texas and northern Mexico, and also over eastern Oklahoma and Kansas (Fig. 1d).

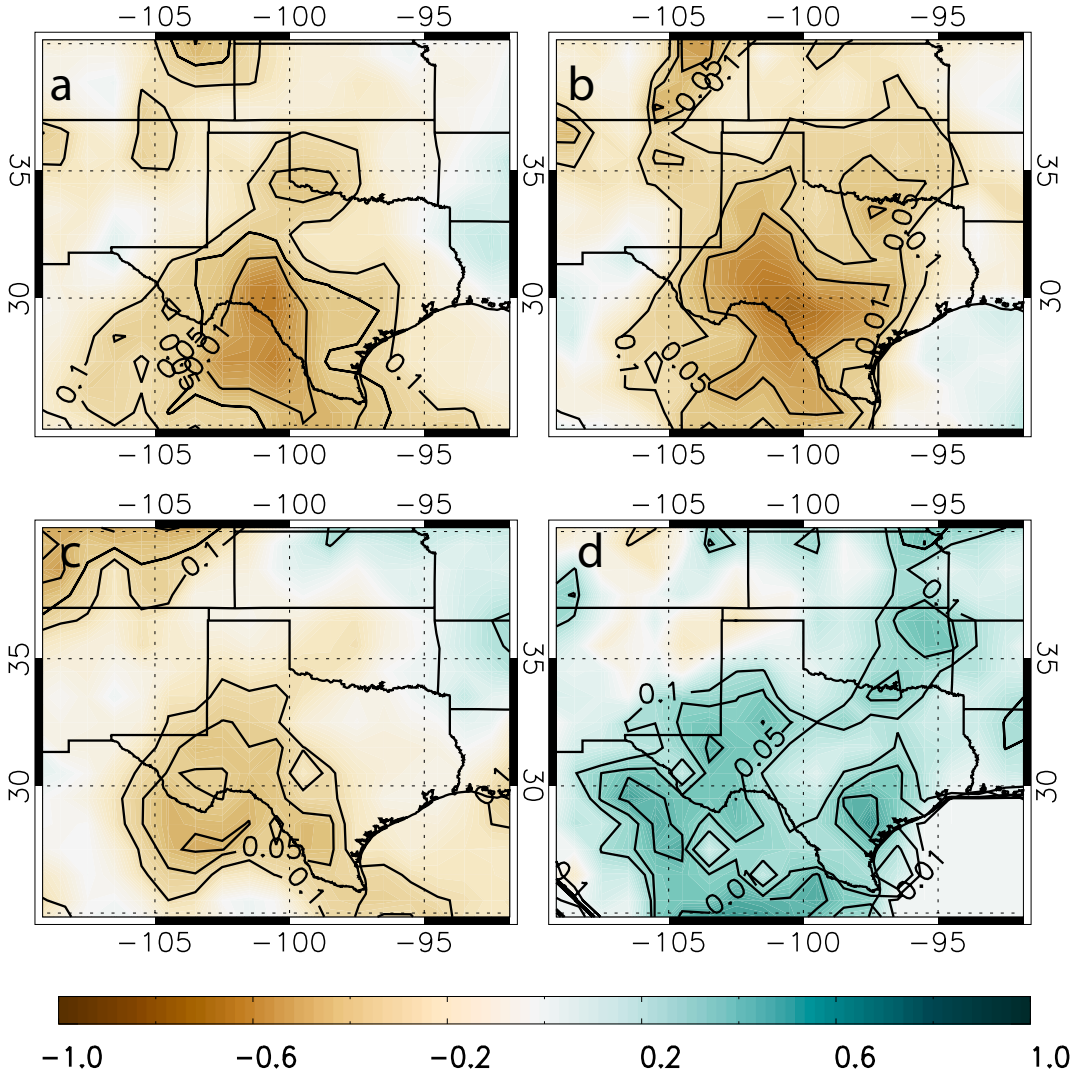

Fig. 1. Spearman's rank correlation between MJJ precipitation (mm/day) and various meteorological parameters, such as (a) 500 hPa geopotential height (m), (b) Surface Temperature (K), (c) CIN, and (d) Soil moisture (kg/m^3) during the month of April over the domain. Brown (green) color represents negative (positive) correlation coefficients (see, color bar). Black line contour represents the p values for significant correlations. (For interpretation of the references to color in this figure legend, the reader is referred to the web version of this article.)

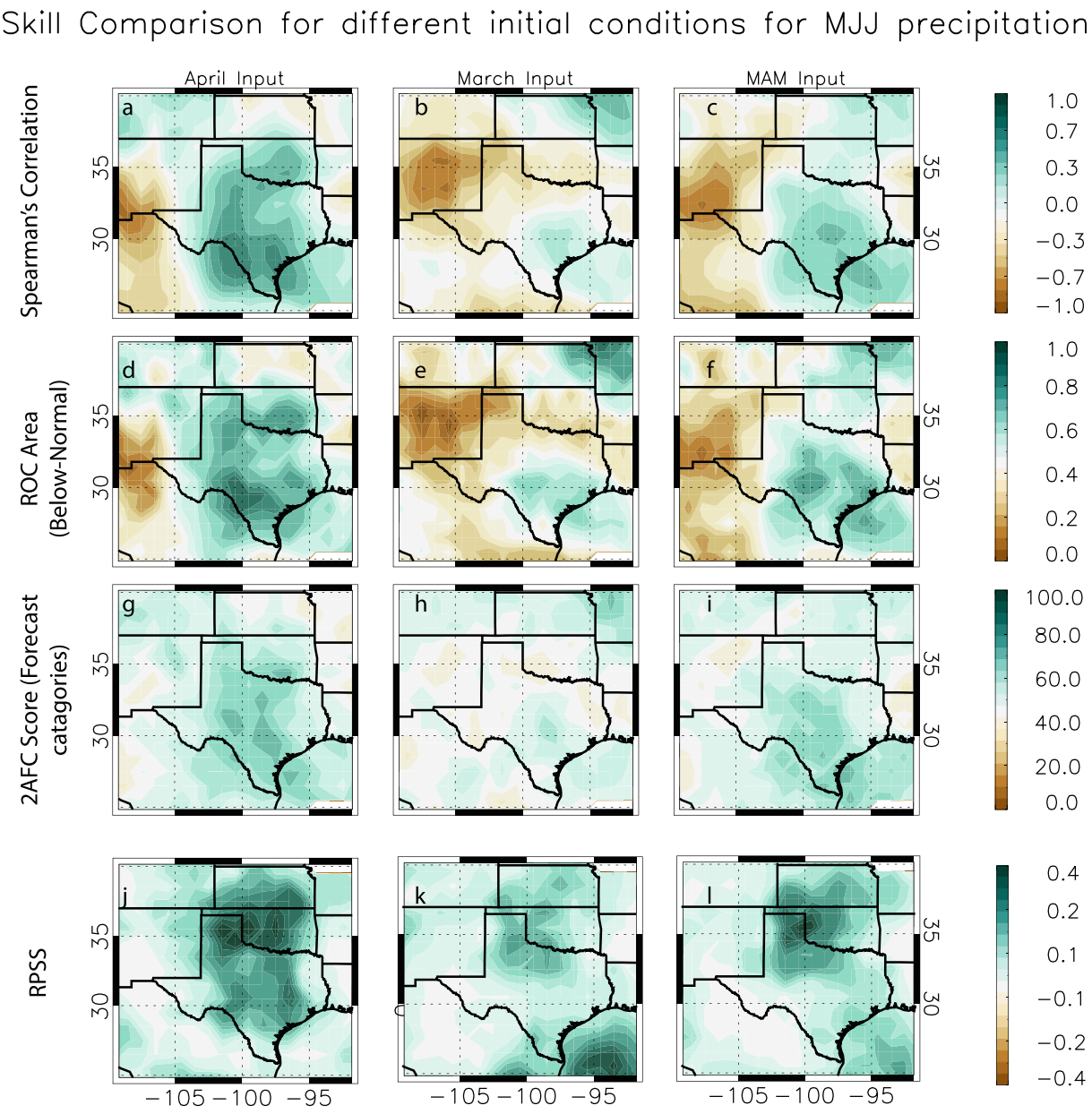

Fig. 2. Comparison of the prediction skills for different initial conditions using April (left column; a, d, g, and j), March (middle column; b, e, h, and k), and MAM (right column; c, f, i, and l) as input time using cross-validated hindcasts between 1982 and 2005 and observations.

In Fig. 2 we show seasonal prediction skills as depicted by the Spearman's Correlation (top panel), ROC (below-normal, second panel), 2AFC (forecast categories, third panel), and RPSS (bottom panel) using April (left column), March (center column) and March through May (MAM, right column), respectively, as the initial conditions for the predictor fields. All the skill metrics show that the best skill is achieved when April initial conditions are used to predict MJJ rainfall. Compared to April, March initial conditions yields poor skills. MAM initial conditions improve prediction skills compared to March-only initial conditions but are still lower than that obtained using April initial conditions. The stronger predictability provided by the anomalous condition shown in Fig. 2 is consistent with the higher sensitive of MJJ drought condition to the anomalous large-scale circulation and land surface conditions in April reported in previous studies (Fernando et al. 2016; Namias 1982)Thus, we use April initial conditions for our analysis in this study.

We also compare the skill of the statistical prediction (Fig. 2) to the dynamical seasonal prediction by the NMME for MJJ rainfall anomalies initialized in April (Fig. 3a–3c). Statistical prediction skills are consistently higher than those of NMME across all three-skill metrics by 20–50% over Texas, Oklahoma, eastern New Mexico and Northeast Mexico. In the northern and western parts of the domain, the dynamical forecast outperforms the statistical forecast. These results are consistent with, and presumably caused by, stronger spring to summer memory and land-atmospheric feedbacks over Texas, Oklahoma, northeastern Mexico and Colorado (Fig. 1). It is interesting to note that RPSS skills are negative, which shows that multi model ensemble members predict exactly opposite to the observation since RPSS is computed from the differences between the observation and prediction.

Decision makers in Texas, such as water resource managers need MJJ rainfall predictions with lead-time of more than one season. Yet, our statistical prediction skill is limited to one season by the intrinsic memory of the climate system. Given better skills of dynamical prediction in winter and early spring (Quan et al. 2012), we investigate if it is feasible to extend the lead-time for the MJJ rainfall forecast using a hybrid statistical-dynamical approach. In Fig. 4 we show skill metrics for longer lead-time forecasts of MJJ rainfall. As expected, prediction

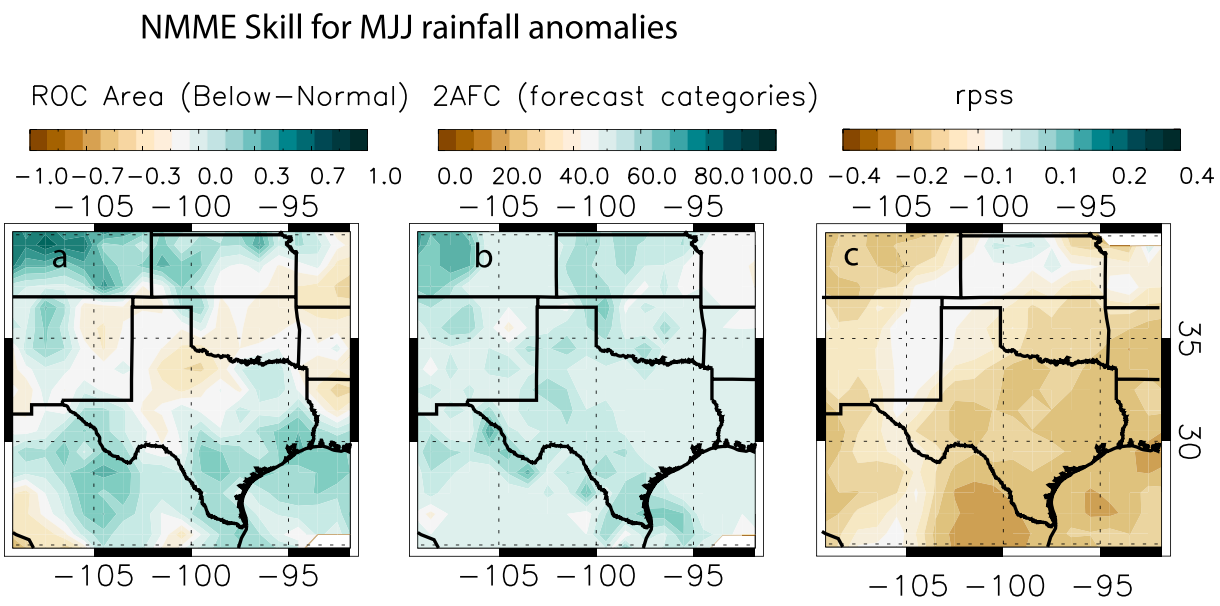

Fig. 3. NMME skill maps for MJJ rainfall anomalies initialized in April.

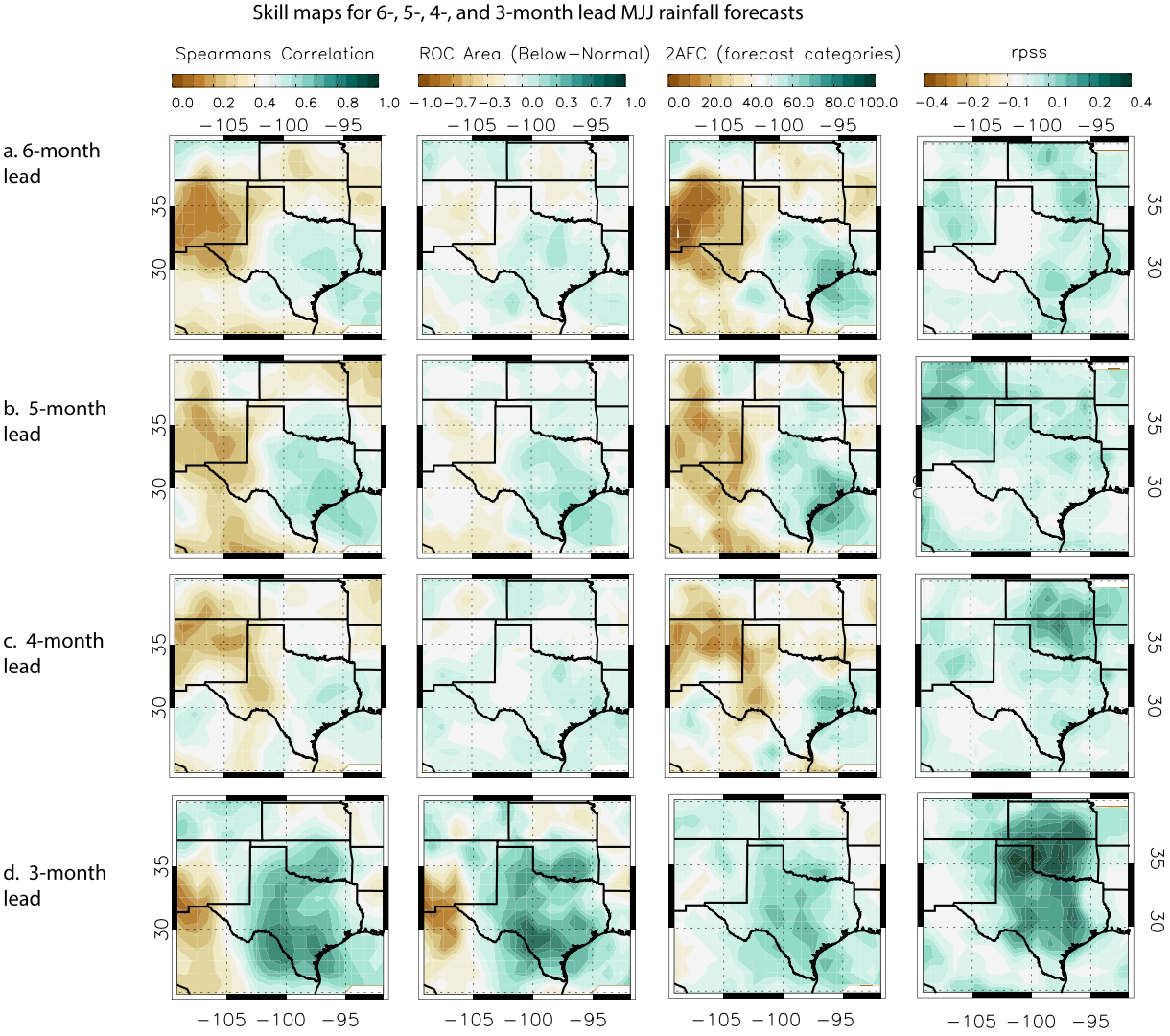

Fig. 4. Skill comparison maps for MJJ rainfall anomalies using initial conditions in (a) January-April (6 months lead), (b), February-April (5 months lead), (c) March and April (4 months lead), and (d) April (4 months lead) .

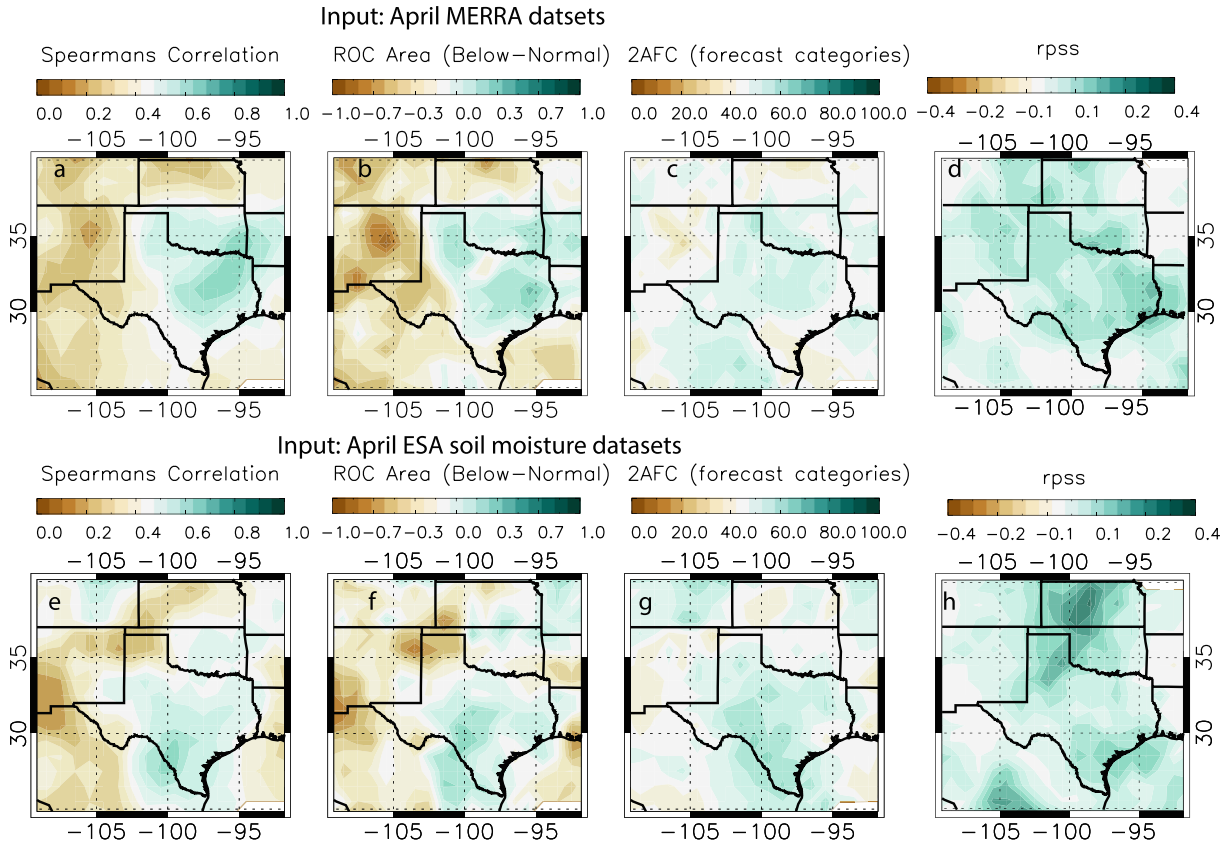

Fig. 5. Skill maps for MJJ rainfall anomalies using initial conditions from MERRA reanalysis product (top panel; a, b, c, and d) and ESA soil moisture datasets (bottom panel; e, f, g, and h) during the month of April.

skill decreases as forecast lead-time increases. However, despite the weakening of atmospheric memory with longer lead-time initial conditions, this hybrid dynamical-statistical prediction system begins to show skills for the probabilistic predictions (>0.5) as early as in February (Fig. 4b, the middle and right panels). Grid points with the highest ROC and 2AFC scores lie within Texas and Oklahoma for the probabilistic forecasts initialized with April inputs (Fig. 4d, middle and right panels). Deterministic forecast skill, RPSS (>0.3), or the Spearman's correlation coefficient is also high (>0.6) when we use April as the initial condition. Thus, the hybrid dynamical-statistical prediction has shown the potential to provide useful information to support decision-making in the water sector.

We have also used other reanalysis datasets to test the sensitivity of the statistical forecast tool to input data sets. In Fig. 5a-5d we show the prediction skill for MJJ rainfall anomalies using predictors fields in April obtained from MERRA. The skills are noticeably lower than those using CFSR for the predictor fields (Fig. 5e-5 h). Fig. 5e-5 h show the prediction skills of the MJJ rainfall anomalies using soil moisture anomalies obtained from ECV-SM datasets to replace soil moisture anomalies obtained from CFSR. The skills are generally lower than those using the CFSR, presumably because the satellite-based soil moisture in ECV-SM represents only surface soil moisture (the top 0.5–2 cm soil layer).

In Fig. 6 we show MJJ rainfall hindcasts at various lead-times for 2011, 2012, 2013, and 2014 using initial conditions of predictor fields in April from CFSR data, and hindcasts of April predictor fields from NMME predictions initialized in January, February, and March, respectively, for 6, 5, and 4-month lead-time rainfall hindcasts. During 2011 (left column), the hindcasts show that the hybrid dynamical-statistical prediction system would be able to predict the early MJJ rainfall deficits with a 6-month lead-time except for the Texas Panhandle, West Texas, New Mexico and the southeastern Colorado (Fig. 6a). The predictions with 5 and 4-month lead-time (Fig. 6e and i) show higher skills than those of NMME predictions with 3-months leadtime (Fig. 3). The statistical prediction system's hindcasts of MJJ rainfall deficits are comparable to those observed (Fig. 6m and 6q) over much of the Southern Great Plains at 3-month lead-time. The hindcasts for 2012 also captures the observed dry rainfall anomalies in MJJ, although they substantially underestimate the rainfall deficits (Fig. 6b, 6f, 6j, 6n, and 6r). The hindcasts mostly missed the observed spatial patterns of the MJJ rainfall anomalies in 2013 (Fig. 6c, g, k, o, and s). In 2014, the hybrid dynamical-statisticalal hindcasts with at 5-month and −4-month lead-times are able to predict the wet anomalies (Fig. 6h, 6i), although it underestimates the magnitude of the observed rainfall anomaly (Fig. 6t). The hybrid dynamical-statistical hindcast for 2014 at the 6-month lead time predicts strong dry anomalies in MJJ (Fig. 6d), opposite as that observed (Fig. 6t). The statistical hindcast of 3- month lead time (Fig. 6p) strongly overestimates the wet MJJ rainfall anomalies compared to the observation (Fig. 6t). Thus, the statistical and hybrid dynamical-statistical prediction systems appear to perform better at predicting strong dry rainfall anomalies (2011) than at predicting weaker dry anomalies (2012) or wetter rainfall anomalies (2014). The dynamical-statistical forecast also failed to accurately predict the spatially mixed dry and wet anomalies over Texas and the Southern Great Plains in 2013. Table 1

We tracked the interest in the drought forecast tool (called "rainfall forecast tool" from May 1, 2017), and the information page on the forecast tool using Google Analytics metrics. We report here (Table 2) on the number of page views and the number of unique views on these tools since they were deployed. Full Google Analytics reports, with the link to the relevant site, are being sent as a separate attachment to this report.

In the first year since the drought (rainfall) tool went online there were 876 unique views on the page. In the second year (May 1, 2017–April 30, 2018) and the start of the third year (May 1–May 31, 2018) there were 966 unique views on the page. This is a 10.27% increase in the second year since the tool was launched. Similarly, there

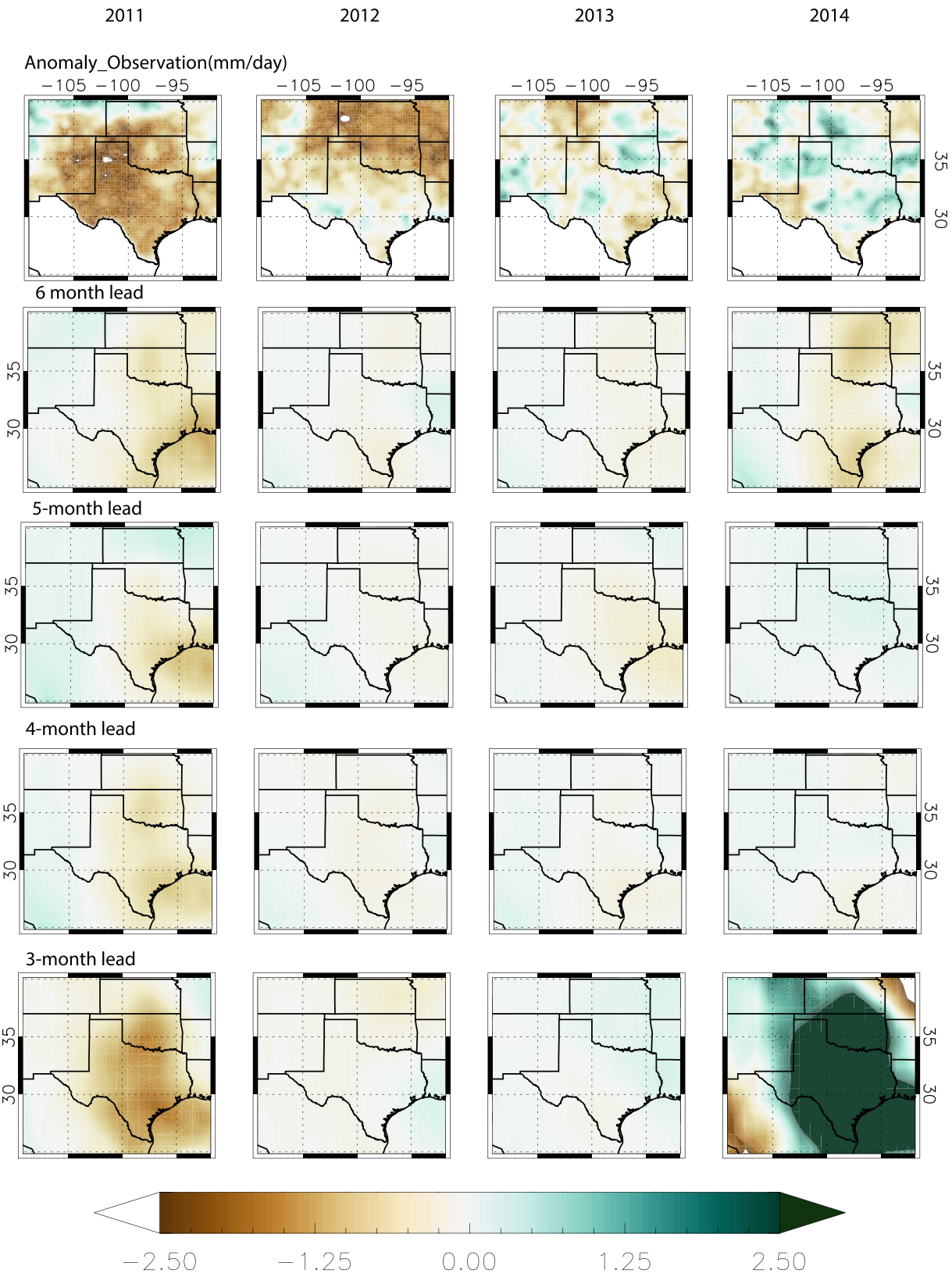

Fig. 6. Maps of statistical forecasts of rainfall anomalies based on initial conditions in (a-d) January (6 months lead), (e-h), February (5 months lead), (i-l) March (4 months lead), and (m-p) April (3 months lead) for 2011–2014. (q-t) observed precipitation anomaly during 2011–2014 using CPC data sets. All anomalies are estimated based on 1982–2010 mean of hindcasts and observation.

was a 60.8% increase in unique views on the drought forecast/rainfall forecast information page in the second year. We interpret this increase in the number unique page views to represent an increased interest in the forecast tool (and its associated information) and an increased adoption of the tool by decision makers as a source of drought early warning information.

Table 1
Lists of data sets used.

Dataset	Period	Parameters	Reference
Climate Forecast System Reanalysis	1982–2010	Geopotential height, pressure, dew point temperature, temperature, soil moisture	Saha et al. 2014
Climate Forecast System version 2	2011–2013	Geopotential height, pressure, dew point temperature, temperature, soil moisture	http://iridl.ldeo.columbia.edu
MERRA (MAIMNPANA); 3 hrly	1982–2013	Geopotential height, pressure, temperature, Relative humidity	https://goldsmr3.gesdisc.eosdis.nasa.gov/opendap/
MERRA (MATMNXLND)	1982–2013	Soil wetness data	https://goldsmr3.gesdisc.eosdis.nasa.gov/opendap/
European Space Agency Climate Change Initiative Essential Climate Variable Soil Moisture (ECV-SM)	1982–2010	Soil Moisture	http://www.esa-soilmoisture-cci.org
CPC global land precipitation dataset	1982–2014	Rainfall	Chen et al. 2002
NMME	1982–2010	CMC1-CanCM3 (10), CMC2-CanCM4 (10), COLA-RSMAS-CCSM3 (6), GFDL-CM2p1-aer04 (10), GFDL-CM2p5-FLOR-A06 (12), NASA-GMAO-062012 (12), and CFSv2 (28).	Kirtman et al., 2014

5. Conclusions and discussion

Rainfall during May-July (MJJ) has strong impacts on agriculture and water resource availability and demand over the Southern Great Plains and Texas. However, predicting MJJ rainfall on the seasonal scale is especially challenging for dynamical weather-climate models over the Southern US Great Plains (Quan et al. 2012). To address this challenge, we have developed a seasonal statistical and a dynamical-statistical prediction system based on the observed relationship between spring anomalous atmospheric and land surface conditions and the MJJ rainfall anomalies reported extensively in the literature. This statistical prediction system is based on CCA (implemented using the IRI's Climate Predictability Tool) and has the three key pre-conditions in spring, i.e. 500 hPa geopotential height, the CIN index determined by the difference in temperature between 700 hPa and dew-point at the surface, and soil moisture anomalies, as the predictor variables and mean MJJ rainfall anomalies as the predictand. The model is trained using observations for the period of 1982–2005. Our analysis shows that the best skill between forecast and observed MJJ rainfall anomalies is achieved by using April initial conditions of these three predictor variables (Fig. 2). The predictand used in this paper is MJJ rainfall anomalies. The rainfall forecast can be provided either as a deterministic forecast of rainfall anomalies or as categorical probabilistic forecasts of the likelihood that MJJ rainfall will be below-, above, or near-normal (e.g. https://waterdatafortexas.org/drought/rainfall-forecast).

The skill of this seasonal statistical prediction system, as measured by the Spearman's correlation coefficient, 2AFC, and ROC, is 20–60% higher than that of the dynamical predictions by NMME (Fig. 3). RPSS also confirm that the best skills for MJJ rainfall prediction are achieved when April initial conditions are used. The highest skill scores are found in Texas, Oklahoma, and northeastern Mexico. Hindcasts outside of the training period show that this prediction system would have predicted the dry rainfall anomalies during MJJ of 2011 with the pattern and magnitude similar to those observed, especially over Texas, Oklahoma, and northeastern Mexico. It also predicted wetter rainfall anomalies during MJJ in 2014, although substantially overestimated their magnitude.

We have also tested the sensitivity of the prediction skills for different reanalysis and soil moisture datasets. The results suggest that the inputs (predictors) derived from the CFSR provide better prediction skills than those from MERRA and ESA-SM soil moisture data.

To address the need for water resource decisions, we further explored a hybrid dynamical-statistical prediction system to predict MJJ rainfall anomalies with 4–6 months lead-time. This hybrid statistical-dynamic prediction system combines the strengths of the dynamical predictions of the large-scale atmospheric circulation and land surface condition in winter and spring with that of the statistical prediction of MJJ rainfall anomalies. It uses the predicted 500 hPa geopotential height, the CIN index, and soil moisture anomalies in April by the NMME predictions initialized in January, February, and March, respectively. This system shows prediction skills up to 3–5 month lead time (Fig. 4). The hindcasts suggest that this hybrid dynamical-statistical prediction system would have predicted the 2011 and 2012 dry rainfall anomalies with up to 3–6-months lead-time. It could also predict the observed wetter anomalies of 2014 with up to 3–5 months' lead-time, although the prediction over-estimates the magnitude.

The combination of the statistical and hybrid statistical-dynamic prediction systems is able to provide an early warning of a drier-than-normal or wetter-than-normal late-spring– early-summer season with lead-time of up to 3–6-months. Given the prediction skills demonstrated by this system, the Texas Water Development Board has been issuing county-level probabilistic rainfall forecasts for the MJJ season in May of 2016 via https://waterdatafortexas.org/drought/rainfall-forecast. These forecasts provide rainfall information, to assist water user groups in the state in their implementation of drought contingency triggers for their water supply sources in the event of an impending MJJ drought. These forecasts provide a window of opportunity for improved forecast skills and predictions (Rodwell and Doblas-Reyes 2009) and have been applied to guide the implementation of drought contingency for water supply reservoirs in Texas. These forecast tools available on Water Data for Texas have been tailored to address climate information needs of reservoir operators in Texas. In doing so, these seasonal rainfall predictions shown in this paper is an example of developing a climate service to fill an information gap and meet to meet climate information needs related to drought from stakeholders in the water sector in Texas.

The statistical prediction system is mainly limited to spring and early summer seasons (April-July) when drought memory is observed. In other seasons, dynamical predictions could out-perform this statistical prediction system, as large-scale dynamics of the atmosphere and oceanic forcing become more important in determining rainfall anomalies.

Table 2
Google Analytics Metrics for tools produced by project.

Tool/information	Time period	Page Views	Unique Page Views
Drought forecast	May 1, 2016–April 30, 2017 (year 1)	1138	876
Drought forecast information page	May 1, 2016–April 30, 2017	215	166
Rainfall forecast	May 1, 2017–May 31, 2018 (year 2 and start of year 3)	1266	966
Rainfall forecast information page	May 1, 2016–April 30, 2017	340	267

Declaration of Competing Interest

The authors declare that they have no known competing financial interests or personal relationships that could have appeared to influence the work reported in this paper.

Acknowledgments

Drought early warning research at the University of Texas at Austin and the University of California Los Angeles is funded by the NASA Indicators for the National Climate Assessment Program (Grants NNX16AN12G, NNX13AN39G), NOAA's Climate Program Office's Modeling, Analysis, Predictions, and Projections Program (Grant Award NA17OAR4310123) and the Jackson School of Geosciences. Drought research at, and the provision of interactive rainfall forecasts to aid Drought Contingency Planning by, the Texas Water Development Board have been funded by the U.S. Army Corps of Engineers Texas Water Allocation Assistance Program (Grant Award W45XMA12285923) and the U.S. Bureau of Reclamation Drought Response Program (Grant Award R15AP00184). The research was also supported by the Postdocs Applying Climate Expertise Postdoctoral Fellowship Program from 2011–2013, which was partially funded by NOAA's Climate Program Office and administered by the University Corporation for Atmospheric Research Visiting Scientist Programs. Links to data sets used in this paper can be found in Table 1. We also extend our thanks to Dr. Bing Pu, Dr. Ying Sun, and Dr. Binyan Yan for their help in this study.

References

Barnston, A.G., Livezey, R.E., 1987. Classification, Seasonality and Persistence of Low-Frequency Atmospheric Circulation Patterns. Mon. Weather Rev. 115, 1083–1126.
Barnston, A.G., Ropelewski, C.F., 1992. Prediction of Enso Episodes Using Canonical Correlation-Analysis. J. Climate 5, 1316–1345.
Barnston, A.G., Vandendool, H.M., 1993. A Degeneracy in Cross-Validated Skill in Regression-Based Forecasts. J. Climate 6, 963–977.
Chen, M.Y., Xie, P.P., Janowiak, J.E., Arkin, P.A., 2002. Global land precipitation: A 50-yr monthly analysis based on gauge observations. J. Hydrometeorol. 3, 249–266.
Christel, I., Hemment, D., Bojovic, D., Cucchietti, F., Calvo, L., Stefaner, M., Buontempo, C., 2018. Introducing design in the development of effective climate services. Clim. Serv. 9, 111–121.
Dai, A., Trenberth, K.E., 2004. The diurnal cycle and its depiction in the Community Climate System Model. J. Climate 17, 930–951.
Eichler, T., Higgins, W., 2006. Climatology and ENSO-related variability of North American extratropical cyclone activity. J. Climate 19, 2076–2093.
Fernando, D.N., Coauthors,, 2016. What caused the spring intensification and winter demise of the 2011 drought over Texas? Clim. Dynam. 47, 3077–3090.
Goddard, L., Dilley, M., 2005. El Nino: Catastrophe or opportunity. J. Climate 18, 651–665.
Hao, Z.C., Singh, V.P., Xia, Y.L., 2018. Seasonal Drought Prediction: Advances, Challenges, and Future Prospects. Rev. Geophys. 56, 108–141.
Hoerling, M., Coauthors,, 2014. Causes and Predictability of the 2012 Great Plains Drought. B. Am. Meteorol. Soc. 95, 269–282.
Hong, S.Y., Kalnay, E., 2002. The 1998 Oklahoma-Texas drought: Mechanistic experiments with NCEP global and regional models. J. Climate 15, 945–963.
Infanti, J.M., Kirtman, B.P., 2014. Southeastern US Rainfall Prediction in the North American Multi-Model Ensemble. J. Hydrometeorol. 15, 529–550.
Kaiser, H.F., 1958. The Varimax Criterion for Analytic Rotation in Factor-Analysis. Psychometrika 23, 187–200.
Kam, J.H., Sheffield, J., Yuan, X., Wood, E.F., 2014. Did a skillful prediction of sea surface temperatures help or hinder forecasting of the 2012 Midwestern US drought? Environ. Res. Lett. 9.
Kirtman, B.P., Min, D., Infanti, J.M., 2014. The North American Multimodel Ensemble: Phase-1 Seasonal-to-Interannual Prediction; Phase-2 toward Developing Intraseasonal Prediction. B. Am. Meteorol. Soc. 95, 585–601.
Koster, R.D., Coauthors,, 2004. Regions of strong coupling between soil moisture and precipitation. Science 305, 1138–1140.
Kousky, V.E., 1989. The Global Climate for September-November 1988: High Southern Oscillation Index and Cold Episode Characteristics Continued. J. Climate 2, 173–192.
Kumar, A., Chen, M.Y., Hoerling, M., Eischeid, J., 2013. Do extreme climate events require extreme forcings? Geophys. Res. Lett. 40, 3440–3445.
Landman, W.A., Mason, S.J., 2001. Forecasts of near-global sea surface temperatures using canonical correlation analysis. J. Climate 14, 3819–3833.
Liu, Y.Y., Coauthors,, 2011. Developing an improved soil moisture dataset by blending passive and active microwave satellite-based retrievals. Hydrol. Earth Syst. Sc. 15, 425–436.
Liu, Y.Y., Coauthors,, 2012. Trend-preserving blending of passive and active microwave soil moisture retrievals. Remote Sens. Environ. 123, 280–297.
Livneh, B., Hoerling, M.P., 2016. The Physics of Drought in the US Central Great Plains. J. Climate 29, 6783–6804.
Lorenz, E. N., 1956. Empirical Orthogonal Functions and Statistical Weather Prediction. Massachusetts Institute of Technology, Department of Meteorology.
Lyon, B., Dole, R.M., 1995. A Diagnostic Comparison of the 1980 and 1988 Us Summer Heat Wave-Droughts. J. Climate 8, 1658–1675.
Mason, S.J., Graham, N.E., 2002. Areas beneath the relative operating characteristics (ROC) and relative operating levels (ROL) curves: Statistical significance and interpretation. Q. J. Roy. Meteor. Soc. 128, 2145–2166.
Mason, S.J., Weigel, A.P., 2009. A Generic Forecast Verification Framework for Administrative Purposes. Mon. Weather Rev. 137, 331–349.
Mason, S. J., Tippet, M. K., 2016: Climate Predictability Tool version 15.3. Columbia University Academic Commons, doi:https://doi.org/10.7916/D8NS0TQ6.
Michaelsen, J., 1987. Cross-Validation in Statistical Climate Forecast Models. J. Clim. Appl. Meteorol. 26, 1589–1600.
Mo, K.C., Lyon, B., 2015. Global Meteorological Drought Prediction Using the North American Multi-Model Ensemble. J. Hydrometeorol. 16, 1409–1424.
Mueller, B., Seneviratne, S.I., 2012. Hot days induced by precipitation deficits at the global scale. P. Natl. Acad. Sci. USA 109, 12398–12403.
Muller, W.A., Appenzeller, C., Doblas-Reyes, F.J., Liniger, M.A., 2005. A debiased ranked probability skill score to evaluate probabilistic ensemble forecasts with small ensemble sizes. J. Climate 18, 1513–1523.
Myoung, B., Nielsen-Gammon, J.W., 2010a. The Convective Instability Pathway to Warm Season Drought in Texas. Part II: Free-Tropospheric Modulation of Convective Inhibition. J. Climate 23, 4474–4488.
Myoung, B., Nielsen-Gammon, J.W., 2010b. The Convective Instability Pathway to Warm Season Drought in Texas. Part I: The Role of Convective Inhibition and Its Modulation by Soil Moisture. J. Climate 23, 4461–4473.
Namias, J., 1982. Anatomy of Great Plains Protracted Heat Waves (Especially the 1980 United-States Summer Drought). Mon. Weather Rev. 110, 824–838.
Pu, B., Fu, R., Dickinson, R.E., Fernando, D.N., 2016. Why do summer droughts in the Southern Great Plains occur in some La Nina years but not others? J. Geophys. Res.-Atmos. 121, 1120–1137.
Quan, X.W., Hoerling, M.P., Lyon, B., Kumar, A., Bell, M.A., Tippett, M.K., Wang, H., 2012. Prospects for Dynamical Prediction of Meteorological Drought. J. Appl. Meteorol. Clim. 51, 1238–1252.
Richman, M.B., 1986. Rotation of Principal Components. J. Climatol. 6, 293–335.
Rienecker, M.M., Coauthors,, 2011. MERRA: NASA's Modern-Era Retrospective Analysis for Research and Applications. J. Clim. 24, 3624–3648.
Rodwell, M. J., Doblas-Reyes, F. J., 2009. Medium-Range, Monthly, and Seasonal Prediction for Europe and the Use of Forecast Information (vol 19, pg 6025, 2006). J. Climate, 22, 3511-3511.
Ropelewski, C.F., Halpert, M.S., 1986. North-American Precipitation and Temperature Patterns Associated with the Elnino Southern Oscillation (Enso). Mon. Weather Rev. 114, 2352–2362.
Ropelewski, C.F., Halpert, M.S., 1987. Global and Regional Scale Precipitation Patterns Associated with the El-Nino Southern Oscillation. Mon. Weather Rev. 115, 1606–1626.
Ryu, J.H., Hayhoe, K., 2017a. Observed and CMIP5 modeled influence of large-scale circulation on summer precipitation and drought in the South-Central United States. Clim. Dynam. 49, 4293–4310.
Ryu, J. H., Hayhoe, K., 2017b: Observed and CMIP5 modeled influence of large-scale circulation on summer precipitation and drought in the South-Central United States (vol 49, pg 4293, 2017). Clim. Dynam. 49, 4311-4311.
Saha, S., Coauthors,, 2014. The NCEP Climate Forecast System Version 2. J. Climate 27, 2185–2208.
Saha, S., Coauthors, 2010. The Ncep Climate Forecast System Reanalysis. B. Am. Meteorol. Soc. 91, 1015–1057.
Schubert, S., Coauthors, 2009. A US CLIVAR Project to Assess and Compare the Responses of Global Climate Models to Drought-Related SST Forcing Patterns: Overview and Results. J. Clim. 22, 5251–5272.
Seager, R., Goddard, L., Nakamura, J., Henderson, N., Lee, D.E., 2014. Dynamical Causes of the 2010/11 Texas-Northern Mexico Drought* J. Hydrometeorol. 15, 39–68.
Shabbar, A., Barnston, A.G., 1996. Skill of seasonal climate forecasts in Canada using canonical correlation analysis. Mon. Weather Rev. 124, 2370–2385.
Simon J. Mason, M. K. T., 2017: Climate Predictability Tool version 15.6.3. Columbia University Academic Commons.
Slater, L.J., Villarini, G., Bradley, A.A., 2016. Evaluation of the skill of North-American Multi-Model Ensemble (NMME) Global Climate Models in predicting average and extreme precipitation and temperature over the continental USA. Clim. Dynam. 1–16.
Steiner, J.L., Briske, D.D., Brown, D.P., Rottler, C.M., 2018. Vulnerability of Southern Plains agriculture to climate change. Clim. Change 146, 201–218.
von Storch, H., Zwiers, F.W., 2002. Statistical analysis in climate research. Cambridge University Press.
Wang, Y.C., Pan, H.L., Hsu, H.H., 2015. Impacts of the triggering function of cumulus parameterization on warm-season diurnal rainfall cycles at the Atmospheric Radiation Measurement Southern Great Plains site. J. Geophys. Res.-Atmos. 120, 10681–10702.
Wilks, D.S., 2006. Statistical Methods in the Atmospheric Sciences, 2nd ed. Academic Press, pp. 463.